

Orientation and alignment parameters in e^\pm impact excitation of hydrogen-like positive ions

Ashok Jain[†], N C Deb[†], N C Sil[‡] and C D Lin[†]

[†] Physics Department, Kansas State University, Manhattan, KS 66506, USA

[‡] Department of Theoretical Physics, Indian Association for the Cultivation of Science, Jadavpur, Calcutta 700032, West Bengal, India

Received 19 April 1988

Abstract. The orientation ($\langle L_y \rangle$) and alignment angle (γ) of the excited 2p state of hydrogen-like positive ions by high-energy electron and positron impact are calculated in the Coulomb-Born approximation. The angular dependence of $\langle L_y \rangle$ and γ is found to be qualitatively similar to the case of e^\pm collisional excitation of the helium atom. We also analyse the shape and rotation of the excited state in terms of the dipole and velocity vectors which result from the coherence between the 2s and 2p levels. The dependence of $\langle L_y \rangle$ and γ on the projectile velocity and target nuclear charge Z is also investigated. Our results reveal that the *classical* grazing model, which interprets positive (negative) $\langle L_y \rangle$ in terms of an attractive (repulsive) force between the projectile and the target, is not valid in general. We also report the orientation and alignment angle for the 3d state of He^+ excited by electron and positron impact.

1. Introduction

There is considerable interest in determining experimentally the shape and rotation of an excited atomic state produced in a collision. In terms of the orientation and alignment parameters, such measurements provide information about the coherence between atomic substates produced in a collision (Fano and Macek 1973, Blum 1981). These measurements also provide complete information on the scattering amplitudes that can be directly compared with quantum mechanical calculations. In the last two decades a number of experimental and theoretical studies on the orientation and the alignment of excited states for different collision systems have been reported (for a comprehensive review and all earlier references, see Andersen *et al* (1988)).

Most of the experimental and theoretical work on the electron impact orientation and alignment parameters has been carried out on neutral atomic targets (mainly on the He atom). Consider the excitation of 2p states in a collision. If the quantisation axis (the z axis) is chosen to be along the direction of the incident beam, and the xz plane is the scattering plane, then only two real parameters are needed to describe the shape and the rotation of the excited 2p states (if pure states are produced in the collision). These two quantities were chosen to be the λ and χ parameters (Eminyan *et al* 1974, Standage and Kleinpoppen 1976), where λ measures the fraction of $2p_0$ scattering probability and χ is the relative phase between the $2p_1$ and $2p_0$ scattering

amplitudes. These two parameters are related directly to the scattering amplitudes. Two alternative parameters, the orientation $\langle L_y \rangle$ and the alignment angle γ , were favoured by Andersen and Hertel (1986). The $\langle L_y \rangle$ is defined to be the expectation value of the angular momentum of the excited electron perpendicular to the scattering plane, while γ is the angle between the major axis of the excited electronic charge cloud and the beam axis, i.e. the alignment angle of the charge cloud. These two parameters offer a more direct physical interpretation of the coherently excited states and will be discussed in this paper.

Experimental and theoretical studies on the orientation of the excited 2p states by electron impact indicate that $\langle L_y \rangle$ is positive at small scattering angles and negative at large angles, with only one sign changeover in between (cf figure 1(a)). This is the characteristic behaviour of $\langle L_y \rangle$ for electron impact excitation of 2p states so long as the collision energy is not too close to the excitation threshold. This general behaviour has been observed for helium and hydrogen targets; it has been found to be true for excitation to higher np ($n > 2$) states as well, both theoretically (Csanak and Cartwright 1986) and experimentally (Eminyan *et al* 1974). These seemingly simple and 'universal' results prompted attempts at physical interpretations using the *classical* grazing model (Kohmoto and Fano 1981, Steph and Golden 1980). In this model, it is argued that at small scattering angles the incident electron does not penetrate the atom and thus it experiences an attractive polarisation potential; consequently, this attractive force is responsible for the electron undergoing a counterclockwise rotation, or a positive

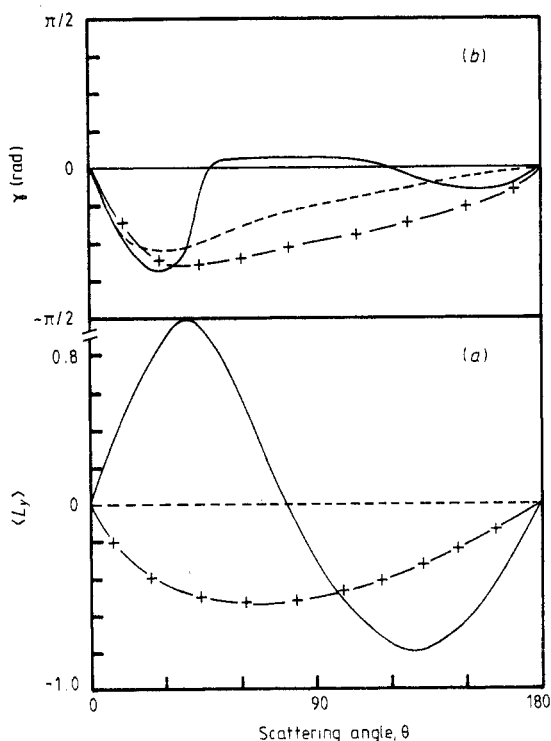


Figure 1. A representative picture of the orientation $\langle L_y \rangle$ (a) and alignment angle γ (b) for electron (—) and positron (---) impact excitation of atomic 2p states of helium atom. The first Born curves are shown by broken curves (Andersen *et al* 1988).

$\langle L_y \rangle$ in the classical sense. For large scattering angles, the incident electron penetrates the atom and experiences a large repulsive force from the electron-electron interaction; this repulsive force is responsible for $\langle L_y \rangle$ being negative at large angles.

This classical grazing model, while it offers a simple interpretation for the sign of $\langle L_y \rangle$ at small and large scattering angles and explains the fact that the results are nearly independent of the target atom, does pose a number of difficulties. Firstly, the effective force between a colliding electron and a neutral atom is always attractive, whether the electron penetrates the atom or not. Secondly, the polarisation potential is *not* the reason for $\langle L_y \rangle$ being positive at small scattering angles. This has been proved by Madison and co-workers (Madison *et al* 1986, Stewart and Madison 1981, Madison and Winters 1983, Bartschat and Madison 1988) in a distorted-wave calculation where they showed that the sign of the orientation parameter was not affected by the inclusion of a polarisation potential. A third, much stronger, piece of evidence for the failure of the classical grazing model comes from the distorted-wave calculation of $\langle L_y \rangle$ for positron impact excitation; the resulting $\langle L_y \rangle$ is negative at all angles. Since the polarisation potential does not depend on the sign of the incident charge (this is true only up to second-order perturbation theory), the classical grazing model would also predict $\langle L_y \rangle$ to be positive for positron excitation at small angles, in contradiction with the results of the distorted-wave calculations.

In this article we examine the orientation $\langle L_y \rangle$ and the alignment angle γ of the excited states of hydrogenic positive ions by electron and positron impact using the Coulomb-Born (CB) approximation. In a way the CB methodology is quite similar to the distorted-wave theory except that the distortion potential is the Coulomb interaction between the incident particle and the positive ion. This force is attractive for incident electrons, and repulsive for incident positrons. We found that the general behaviour of the resulting orientation and alignment parameters, thus calculated, is similar to that obtained for neutral atomic targets. This provides further evidence that the attractive or repulsive forces are not responsible for the change of sign of $\langle L_y \rangle$ in electron impact excitation.

There are many calculations of the cross sections for electron impact excitation of hydrogen-like positive ions at high energies based on various versions of first-order distorted-wave theory (Coulomb-Born-type approximations; see Deb *et al* (1983) and references therein). To the best of our knowledge, the only calculations of the alignment and orientation parameters for the excited states of hydrogenic ions by charged particles are those of Madison *et al* (1986) with results for $\langle L_y \rangle$ in the case of electron impact excitation of the 2^2P state of He^+ and Li^{2+} ions at 100 eV.

This paper has four goals. First, to investigate the θ (scattering angle) dependence of $\langle L_y \rangle$ and γ for excitation of $\text{He}^+(1s-nl)$ by electrons and positrons with impact energy $E = XE_{\text{th}}$ (where E_{th} = threshold energy = $Z^2(1 - 1/n^2)/2$, Z = target nuclear charge, n = principal quantum number of the excited state and X is a number greater than one). Second, to obtain similar information on the orientation and alignment of the excited charge cloud by using the dipole moment and velocity vectors to study the $2s-2p$ coherence (for details of this procedure see Burgdörfer (1983), Burgdörfer and Dube (1984) and Jain *et al* (1987a, b, 1988); see also van Wyngaarden and Walters (1986)). Third, to see how the angular dependence of $\langle L_y \rangle$ and γ changes (*a*) with the nuclear charge Z of the target and (*b*) with E . Fourth, to seek a physical interpretation of these results for positive ions.

In the next section, we review the theoretical model employed to determine the transition amplitudes and we define the various correlation and coherence parameters

reported in this work. Sections 3 and 4 are devoted to the discussion of the results and final conclusions, respectively. We use atomic units throughout.

2. Theory

2.1. Calculation of scattering amplitudes

Since we are concerned here with the orientation and alignment parameters for excitation of hydrogen-like positive ions by high-energy electron and positron impact, we use the basic Coulomb-Born approximation without including exchange effects between the target and projectile electrons (for the positron case there is no such exchange interaction). For the transition $1s \rightarrow nlm$ let the scattering amplitude at an impact energy E be $f_{1s, nlm}(\theta)$. We will express E as X (where $X > 1$) times the excitation threshold energy E_{th} . According to Deb and Sil (1983),

$$f_{1s, nlm}(\theta) = -\frac{1}{2\pi} \iint \phi_{nlm}(\mathbf{r}_2) \psi_{\mathbf{K}_f}^{(-)*}(\mathbf{r}_1) \left(\frac{q}{r_{12}} - \frac{Z_T q}{r_1} \right) \phi_{1s}(\mathbf{r}_2) \psi_{\mathbf{K}_i}^{(+)}(\mathbf{r}_1) d\mathbf{r}_1 d\mathbf{r}_2 \quad (1)$$

where

$$\psi_{\mathbf{K}_i}^{(+)}(\mathbf{r}_1) = \exp\left(q\pi \frac{Z-1}{2K_i}\right) \Gamma(1-a) \exp(i\mathbf{K}_i \cdot \mathbf{r}_1) F_1(a, 1; i(K_i r_1 - \mathbf{K}_i \cdot \mathbf{r}_1)) \quad (2a)$$

$$\psi_{\mathbf{K}_f}^{(-)}(\mathbf{r}_1) = \exp\left(q\pi \frac{Z-1}{2K_f}\right) \Gamma(1+b) \exp(i\mathbf{K}_f \cdot \mathbf{r}_1) F_1(-b, 1; -i(K_f r_1 + \mathbf{K}_f \cdot \mathbf{r}_1)) \quad (2b)$$

with $a = iq(Z-1)/K_i$, $b = iq(Z-1)/K_f$, $q = +1$ for e^- and $q = -1$ for e^+ . \mathbf{K}_i and \mathbf{K}_f are momentum vectors in the initial and final channels respectively.

The functions $\phi_{nlm}(\mathbf{r})$ are hydrogen-like wavefunctions given by,

$$\phi_{nlm}(\mathbf{r}) = A(n, l, \lambda) \sum_{k=0}^{n-l-1} B(n, l, k, \lambda) \exp(-\lambda_f r) r^{k+l} Y_{lm}(\hat{r}) \quad (3)$$

where

$$A(n, l, \lambda) = \left((2\lambda)^3 \frac{(n-l-1)!}{2n[(n+l)!]^3} \right)^{1/2} (2\lambda)^l$$

$$B(n, l, k, \lambda) = \frac{(-1)^{k+2l+1} [(n+l)!]^2 (2\lambda)^k}{(n-l-1-k)! (2l+1+k)! k!}$$

and $\lambda = Z/n$.

The way the $f_{1s, nlm}(\theta)$ are evaluated is described in Deb and Sil (1983). Note that in contrast to the first Born approximation, the CB scattering amplitudes for electron and positron impact differ by more than a phase factor. The scattering plane x - z is defined by the initial and final wavevectors \mathbf{K}_i and \mathbf{K}_f respectively. The axis of quantisation is chosen along \mathbf{K}_i .

It has been shown by Deb *et al* (1983) that when the CB approximation is used for electron impact excitation of $\text{He}^+(1s \rightarrow 2p)$ the total and differential cross sections and the Fano-Macek alignment parameter $A_0^{\text{col}} = (\sigma_{p_0} - \sigma_{p_1}) / (2\sigma_{p_1} + \sigma_{p_0})$ are in good agreement with the results of other high-energy approximations. Here σ_{p_0} and σ_{p_1} are the cross sections for excitation of the $2p_0$ and $2p_1$ sublevels, respectively. We use the scattering amplitudes from the CB approximation to determine the orientation and alignment parameters in this paper.

2.2. Alignment and orientation parameters

The orientation and alignment of 2p states populated in a collision can be determined experimentally by measuring the polarisation of the 2p-1s radiation (Fano and Macek 1973, Blum 1981) or the angular distribution of the emitted photons. In particular, to determine the sign of the orientation parameter $\langle L_y \rangle$ uniquely, the circular polarisation of the emitted radiation has to be measured. Such measurements can be used to 'reconstruct' the scattering amplitudes and the wavefunctions of the 2p states which are populated in the collision. In other words, the coherence between the 2p magnetic substates can be determined. To find out the coherence between the degenerate hydrogenic 2s and 2p states, one has to measure the polarisation (or the Stokes parameters) of the emitted radiation in an external electric field (see, for example, Havener *et al* 1986).

We first consider the 2p part of the wavefunction immediately after the collision (the common time-dependent exponential term is ignored here since it does not appear in the coherence parameters),

$$\Psi_{pp}(\mathbf{r}; \theta) = f_{2p_0}(\theta)\phi_{2p_0}(\mathbf{r}) + f_{2p_1}(\theta)\phi_{2p_1}(\mathbf{r}) + f_{2p_{-1}}(\theta)\phi_{2p_{-1}}(\mathbf{r}). \quad (4)$$

For simplicity we replace $f_{1s, nlm}$ by f_{nlm} .

In (4), we assume that the 2p states are produced as pure states where, for example, there is no contribution from the cascade of higher states populated in the collision. For the np states produced in a collision, due to the symmetry with respect to the collision plane, $f_{np_{-1}} = -f_{np_1}$. Since the absolute phases in the scattering amplitudes are not important, only three real parameters are needed to specify the coherences between np sublevels. If the total probability for excitation to the np states is normalised to unity, then only two real parameters are required. Following the recommendation of Andersen *et al* (1988), these two quantities are chosen to be the orientation, $\langle L_y \rangle$, and the alignment angle, γ . The former specifies the rotation of the electronic charge cloud, while the latter is the angle of the major axis of the electronic charge cloud with respect to the beam axis. $\langle L_y \rangle$ is defined as follows:

$$\langle L_y \rangle = \langle \Psi_{pp}(\mathbf{r}) | L_y | \Psi_{pp}(\mathbf{r}) \rangle = 2\sqrt{2} \operatorname{Im}(f_{2p_0} f_{2p_1}^*) \quad (5)$$

and γ is obtained from the condition

$$\frac{d}{d\gamma} |\Psi_{pp}(\mathbf{r})|^2 = 0$$

(here \mathbf{r} is restricted to the collision plane) which gives

$$\tan(2\gamma) = -2\sqrt{2} \operatorname{Re}(f_{2p_0} f_{2p_1}^*) / (\sigma_{p_0} - 2\sigma_{p_1}). \quad (6)$$

It is, however, more convenient to write $\langle L_y \rangle$ (equation (5)) and γ (equation (6)) in terms of $\lambda = \sigma_{p_0} / (\sigma_{p_0} + 2\sigma_{p_1})$ and $\chi = \chi_1 - \chi_0$, where $f_{2p_0} = |f_{2p_0}| e^{ix_0}$ and $f_{2p_1} = |f_{2p_1}| e^{ix_1}$, namely

$$\langle L_y \rangle = -2[\lambda(1-\lambda)]^{1/2} \sin \chi \quad (7)$$

and

$$\tan(2\gamma) = -2[\lambda(1-\lambda)]^{1/2} \cos \chi / (2\lambda - 1). \quad (8)$$

Note that the corresponding alignment angle in the Born approximation is given by

$$\tan \gamma_{\text{FBA}} = \frac{\sin \theta}{(\cos \theta - [E/(E - \Delta E)]^{1/2})} \quad (9)$$

where ΔE is the excitation energy.

2.3. 2s and 2p coherences

In the case of the 2s-2p coherences, one can extract from the full density matrix of the excited $n = 2$ manifold two simple physical parameters: the dipole moment $\langle \mathbf{D}(\theta) \rangle$ and the velocity vector $\langle (\mathbf{L} \times \mathbf{A})(\theta) \rangle$ at each scattering angle (Burgdörfer 1983, Burgdörfer and Dube 1984, Jain *et al* 1987a, b, 1988). Here \mathbf{A} is the Runge-Lenz vector which is proportional to the dipole moment \mathbf{D} . To include the 2s-2p coherence, the wavefunction for the $n = 2$ level is written as

$$\Psi_{\text{sp}}(\mathbf{r}; \theta) = f_{2s}(\theta)\phi_{2s}(\mathbf{r}) + f_{2p_0}(\theta)\phi_{2p_0}(\mathbf{r}) + f_{2p_1}(\theta)\phi_{2p_1}(\mathbf{r}) + f_{2p_{-1}}(\theta)\phi_{2p_{-1}}(\mathbf{r}). \quad (10)$$

From the wavefunction (equation (10)) the expectation values of $\langle \mathbf{A} \rangle$ and of $\langle (\mathbf{L} \times \mathbf{A}) \rangle$ can be obtained as follows (Burgdörfer 1983):

$$\langle A_x(\theta) \rangle = -2\sqrt{2} \operatorname{Re}(f_{2s}f_{2p_1}^*) \quad (11)$$

$$\langle A_z(\theta) \rangle = 2 \operatorname{Re}(f_{2s}f_{2p_0}^*) \quad (12)$$

$$\langle (\mathbf{L} \times \mathbf{A})_x(\theta) \rangle = -2\sqrt{2} \operatorname{Im}(f_{2s}f_{2p_1}^*) \quad (13)$$

$$\langle (\mathbf{L} \times \mathbf{A})_z(\theta) \rangle = -2 \operatorname{Im}(f_{2s}f_{2p_0}^*). \quad (14)$$

Note that for higher n values, the expressions for \mathbf{A} and $(\mathbf{L} \times \mathbf{A})$ are more complicated.

3. Results and discussion

It is well known that in the first Born approximation (FBA) the orientation parameter vanishes identically (see figure 1(a)) but that γ is non-zero and negative at all scattering angles (see figure 1(b) and Andersen *et al* 1988). Similarly, the dipole moment vector (or $\langle \mathbf{A} \rangle$) is always zero in the FBA, while the velocity vector $\langle (\mathbf{L} \times \mathbf{A}) \rangle$ is not (there is a phase difference of 90° between the FBA 2s and 2p scattering amplitudes). Deviations from these simple results would give indications of the failure of the FBA. For electron impact excitation of neutral atoms, such deviations have been predicted reasonably well in the distorted-wave Born approximation (Madison *et al* 1986). For positive-ion targets, we use the Coulomb-Born approximation to calculate the orientation parameter and the alignment angle.

3.1. Orientation and alignment angle for excitation to 2p states

We first discuss our e^\pm -He $^+$ results at energies from two to five times threshold. Figure 2 displays $\langle L_y \rangle$, γ , λ and χ (plotted as $\sin \chi$) for both electrons (e^-) and positrons (e^+) at $X = 2$ and 4 as functions of scattering angle from 0 to 180° . For the e^+ case, $\langle L_y \rangle$ is always negative, while for e^- scattering $\langle L_y \rangle$ changes sign at middle angles. The crossing angles (to be denoted as θ_0) where $\langle L_y \rangle$ is zero become smaller with increasing energy. This general behaviour is similar to the results for 2p excitation of neutral hydrogen and helium atoms by electron and positron impact. At small scattering angles the alignment angle is negative for both electron and positron collision. As θ increases, the γ for the positron reaches a large negative value before it approaches zero monotonically at large scattering angles. For electrons, γ can reach near-zero values at middle angles. At $X = 2$, it even becomes positive before it becomes negative again at large scattering angles. However, for $X = 4$, the angle γ is always negative. We also note that the change in sign of $\langle L_y \rangle$ for electron impact is due to the value of $\sin \chi$

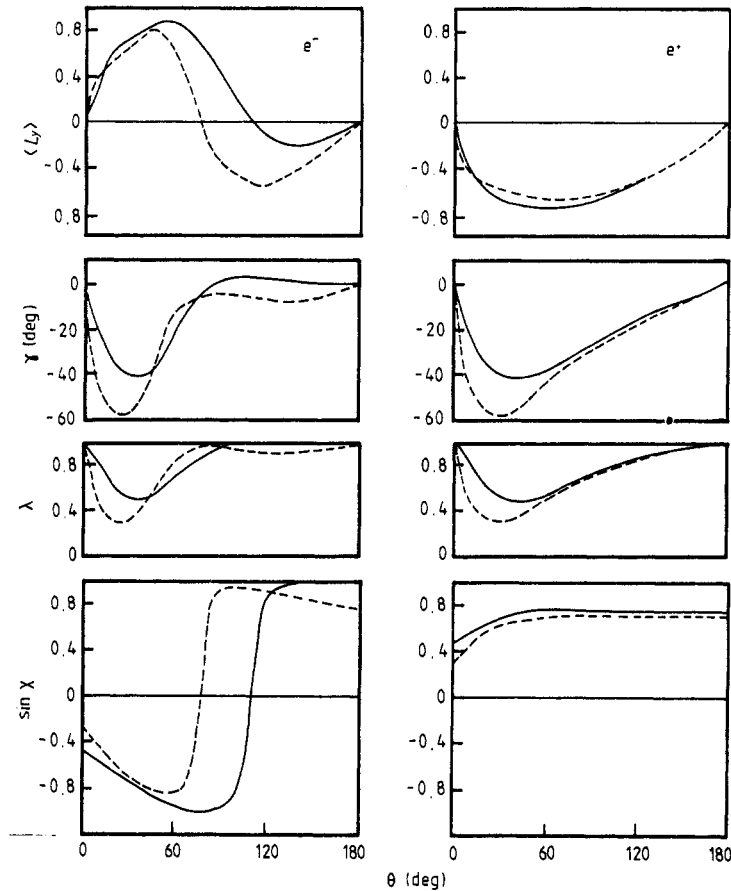


Figure 2. $\langle L_y \rangle$, γ , λ and $\sin \chi$ parameters as functions of the scattering angle θ for the excitation of $\text{He}^+(2p)$ by electrons and positrons at two energies: $E = 2E_{th}$ (full curves) and $E = 4E_{th}$ (broken curves).

which passes through zero at θ_0 . The λ parameter lies between 0 and 1 and it does not play any role in the sign change of $\langle L_y \rangle$.

3.2. The s - p coherence

A set of complementary information about the shape and the rotation of the excited states can be obtained from the coherence of $2s$ and $2p$ states. In figure 3 we show $\langle \mathbf{D} \rangle$ (which is proportional to $\langle \mathbf{A} \rangle$) and $\langle (\mathbf{L} \times \mathbf{A}) \rangle$ vectors as functions of θ at $X = 2$ and $X = 4$. The expectation value of $\langle \mathbf{D} \rangle$ gives the direction of the dipole moment which can be compared with the angle γ derived solely from the coherence of $2p$ states. The alignment angle (γ_{sp}) that can be deduced from the dipole moment picture is calculated from

$$\gamma_{sp} = \tan^{-1}(\langle A_x \rangle / \langle A_z \rangle). \quad (15)$$

Furthermore, if we assign $\langle (\mathbf{L} \times \mathbf{A}) \rangle$ a classical meaning by assuming it to be equal to $\langle \mathbf{L} \rangle \times \langle \mathbf{A} \rangle$ then, knowing $\langle \mathbf{A} \rangle$, we can infer $\langle L_y \rangle$ from the coherence of the $2s$ and $2p$

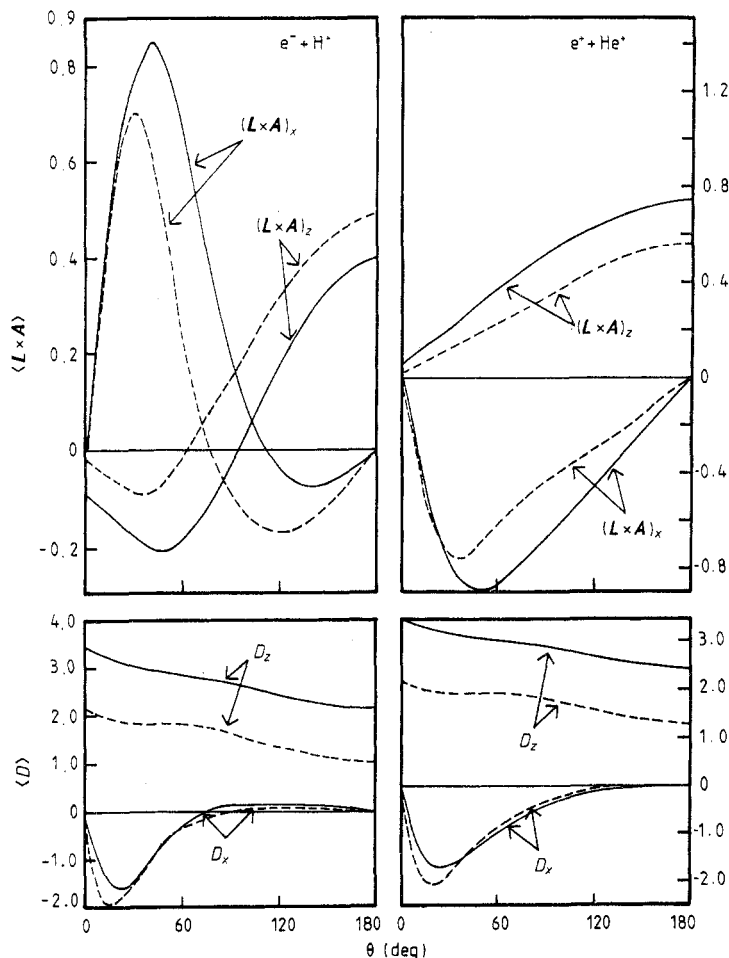


Figure 3. Same as figure 2, but for the dipole (D_x and D_z) and the velocity (x and z components of $(L \times A)$) vectors.

states. The inferred values can be then be compared with those obtained from the study of $2p$ coherence alone.

In figure 4 we compare the angles γ and γ_{sp} for both electron and positron impact. We note that there is general agreement except in the case of electrons at larger scattering angles. Note that the two angles are obtained from completely different quantum mechanical expectation values and there is no *a priori* reason for them to agree.

From the values of $\langle L_y \rangle$ and γ one can construct a classical orbital picture for the motion of the excited electron. This is shown in the upper half of figure 5 for typical results at large and small scattering angles. The angle γ determines how the ellipse is tilted, and the sense of rotation of the electron depends on the sign of $\langle L_y \rangle$. One can obtain a similar *classical* orbital picture of the electron from the dipole moment and the expectation value of $\langle (L \times A) \rangle$ (Jain *et al* 1987a, b, 1988). We note that $\langle (L \times A) \rangle$ is interpreted as the velocity vector at perihelion; together with $\langle A \rangle$ it also gives the sense of rotation of the electron. The results from figure 3 gives the classical orbital pictures shown in the lower half of figure 5. Note that the derived sense of rotation

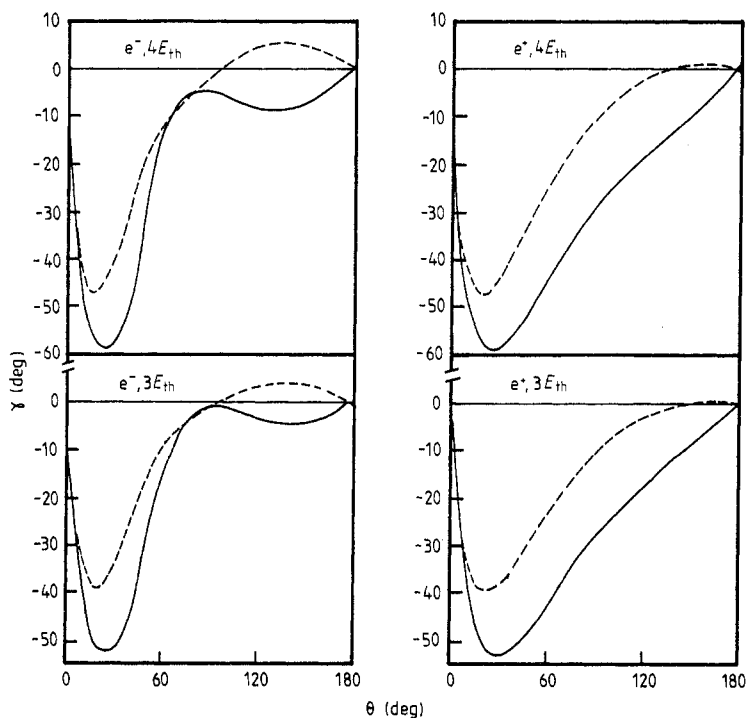


Figure 4. Alignment angles γ (derived from equation (6), full curves) and γ_{sp} (equation (15), broken curves) for electrons and positrons at energies of $3E_{th}$ and $4E_{th}$.

is identical to that shown derived from $\langle L_y \rangle$. Again, we emphasise that the classical pictures given in figure 5 were derived from calculations based on entirely different quantum mechanical operators and there is no *a priori* reason to expect that they should always be consistent.

3.3. The shape of the electronic charge cloud

Another method of directly displaying the orientation of the collisionally populated excited states is to exhibit the surface charge density $|\Psi|^2$ (or its square root, i.e. $|\Psi|$) on the collision plane. This can be done using the wavefunctions including only the 2p states (equation (4)), or the wavefunctions including both 2s and 2p states (equation (10)). In figure 6, we show contour plots of $|\Psi|$ at a number of scattering angles for electron impact. We note that the major axis of the charge cloud derived from 2p alone is quite close to the direction of the electric dipole moment at small scattering angles. At large scattering angles there is some discrepancy. In figure 7 similar results for positron scattering are shown. The direction of the major axis from the 2p states and the direction of the dipole moment from the 2s and 2p states are in general agreement. These plots are consistent with the comparison of γ and γ_{sp} displayed in figure 4.

3.4. Nuclear charge dependence of the orientation parameter

In figure 8 we show the behaviour of $\langle L_y \rangle$ as a function of target nuclear charge Z for $Z = 2, 4$ and 6 at $3E_{th}$ impact energy by electrons. Notice that this impact energy is

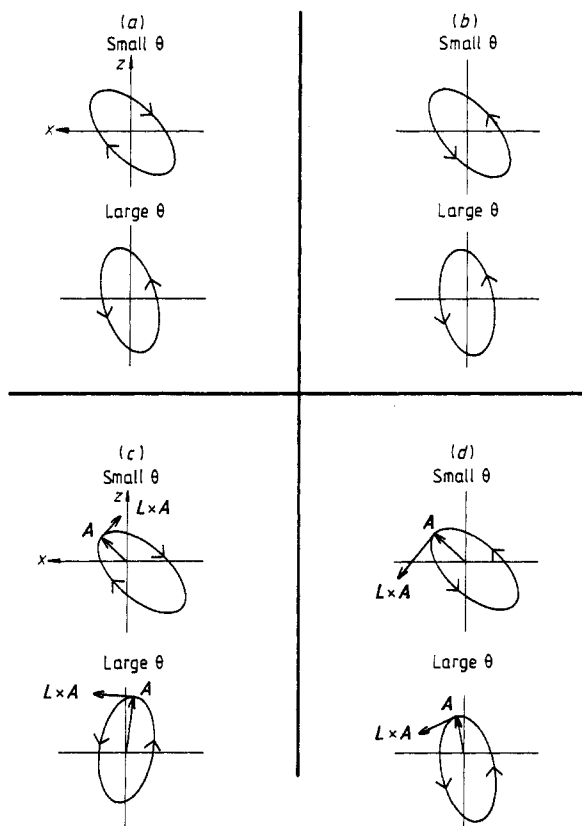


Figure 5. Classical orbital pictures of the electronic charge cloud of the 2p state of He^+ excited by electrons and positrons in the smaller and large angular regions. (a) e^- case using coherence between p states; (b) same as in (a), but for the e^+ case; (c) e^- case using the s-p coherent parameters (for details, see the text); (d) same as in (c) but for e^+ scattering.

different for different targets since E_{th} depends on the Z value of the target. We note that the general shape of the orientation is almost identical and that the angle θ_0 is almost independent of Z (including $Z = 3$ and 5 , not shown). Qualitative scaling of θ_0 with respect to the collision speed and the target charge Z will be addressed elsewhere (Lin and Jain 1988).

The 'universal' behaviour of $\langle L_y \rangle$ for the excitation of 2p states by electron impact for different targets at different energies is astonishing. Such a simplicity has attracted attempts at a simple interpretation in terms of elementary classical concepts. As discussed in the introduction, the classical grazing model attempts to attribute a positive alignment to an attractive effective force between the incident electron and the target and the negative orientation to the repulsive force at close encounters. This simple model contradicts the present results shown in figure 8 where the force between the incident electron and positive ion is expected to be attractive at all distances.

We remark that it appears that our results in figure 8 are in disagreement with the distorted-wave calculation of Madison *et al* (1986) who showed that the $\langle L_y \rangle$ for electron impact on Li^{2+} at 100 eV gives a positive $\langle L_y \rangle$ at *all* scattering angles. This discrepancy is due to the fact that their calculations were done at too low an energy (the excitation energy for $1s \rightarrow 2p$ in Li^{2+} is 93.6 eV). We have made a CB calculation

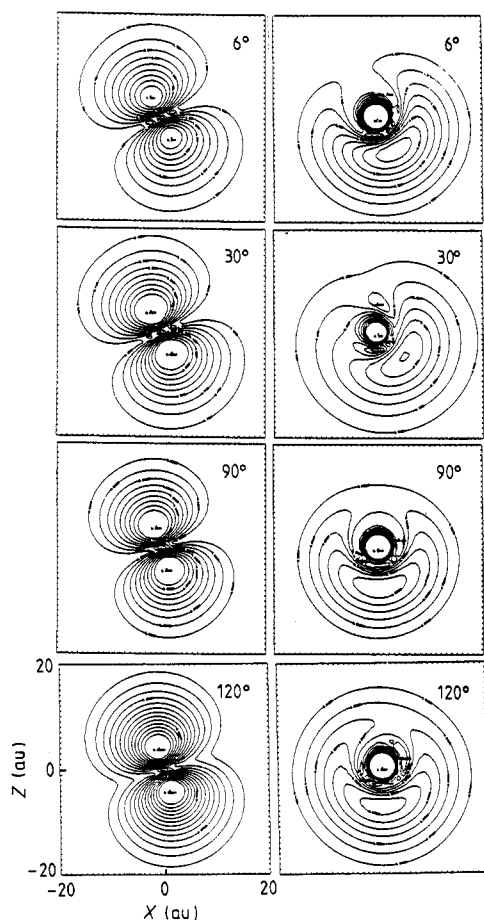


Figure 6. Contour plots of the quantities $|\Psi_{pp}|$ (equation (4), left-hand set of curves) and $|\Psi_{sp}|$ (equation (10), right-hand set of curves) for electron impact excitation of the 2p state of He^+ at $\theta = 6, 30, 90$ and 120° .

at the same energy and confirm the results reported in Madison *et al.* The results shown in figure 8 are typical of collisions at higher energies.

3.5. Orientation and alignment for excitation to 3d states

There are few measurements of the orientation and alignment of nd states. Andersen *et al.* (1983) have measured and discussed the $s \rightarrow d$ excitation in Li-He collisions. Very recently, Beijers *et al.* (1987) have measured the circular polarisation P_3 (this is proportional to $\langle L_y \rangle$ but has the opposite sign) of the light emitted from the decay of the 3^1D state of the excited He atom by 40 eV electrons between 30 and 60°. An interesting outcome of this experiment is that $\langle L_y \rangle$ is negative at these (intermediate) angles in contrast to 3^1P (or 2^1P) for which $\langle L_y \rangle$ is positive in this angular range. The first-order many-body perturbation theory (FOMBT-SCF) calculations of Cartwright and Csanak (1987) confirm these experimental results approximately, but the distorted-wave Born approximation (DWBA) calculations of Bartschat and Madison (1988) do not. In the so-called DWBA-EP model, where the excited-state potential is used to calculate the distortion of the wavefunctions, Bartschat and Madison (1988) obtained orientation

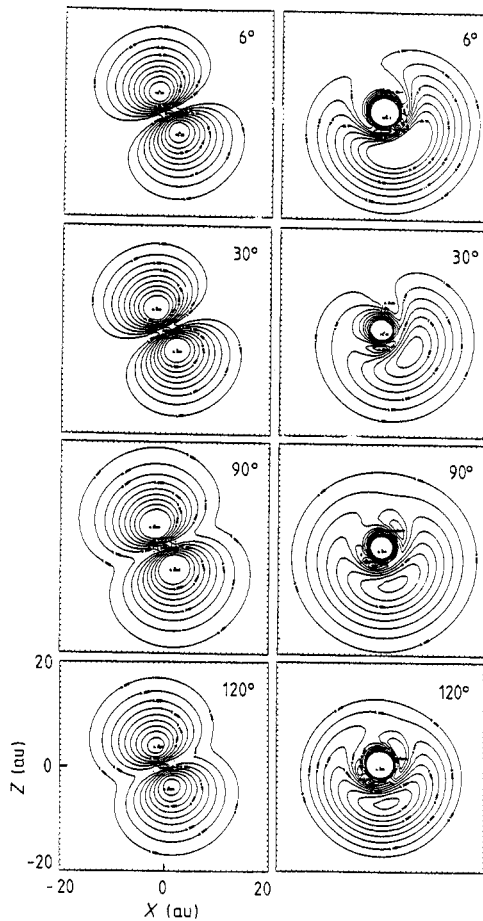


Figure 7. Same as figure 6, but for positron impact excitation.

parameters which are quite different from experiment (even the sign is wrong). On the other hand, with the DWBA-GP model, where the distortion potential is that of the initial state, the results were in better agreement with experiment. The difficulty arises since the DWBA-EP model was found to be in better agreement in describing the excitation of np states. We note, however, that the energy used by Bartschat and Madison (i.e. 40 eV) may be too small for these first-order distorted-wave models to be valid.

In order to see if there is some general energy dependence of the orientation parameter for electron impact excitation of 3d states, we calculated $\langle L_y \rangle$ for excitation of the 3d states of He^+ at four energies ($X = 2, 2.5, 3$ and 5) using the Coulomb-Born approximation. The results are shown in figure 9. It is clear that the energy dependence of the d state $\langle L_y \rangle$ is not as well behaved as in the excitation of np states. Similar strong energy dependence of $\langle L_y \rangle$ was found in the excitation of the 3^1D state of helium by electron impact in the calculation of Cartwright and Csanak (1987).

The expression of $\langle L_y \rangle$ for 3d is more complicated than for np states. In terms of scattering amplitudes,

$$\langle L_y \rangle = 4 \text{Im}(\sqrt{\frac{3}{2}} f_{3d_0} f_{3d_1}^* + f_{3d_1} f_{3d_2}^*). \quad (16)$$

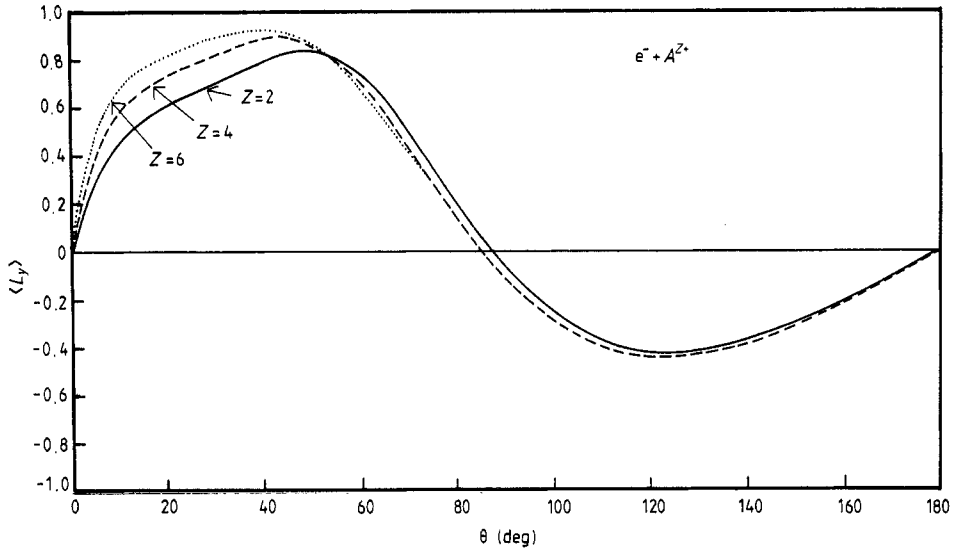


Figure 8. Z dependence of the $\langle L_y \rangle$ parameter at $3E_{th}$ energy.

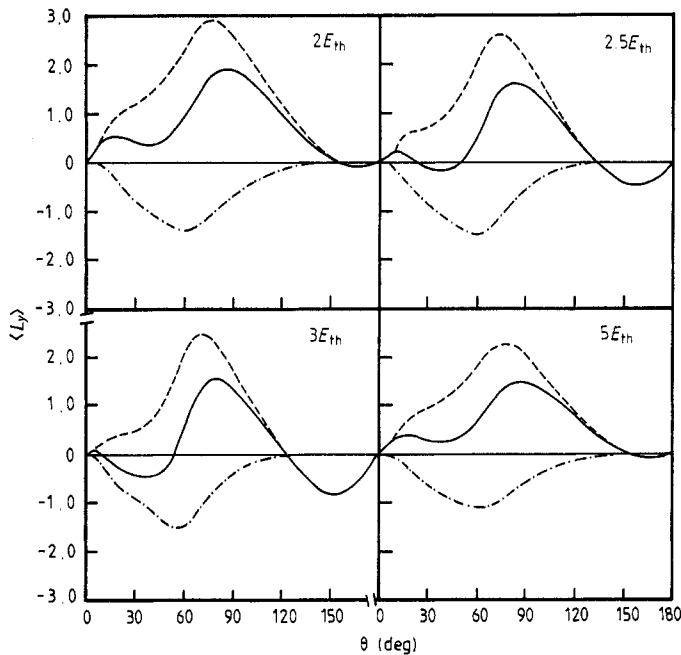


Figure 9. $\langle L_y \rangle$ parameter for the excitation of the 3d state of He^+ by electron impact at $2E_{th}$, $2.5E_{th}$, $3E_{th}$ and $5E_{th}$ impact energies. The full curve represents the sum of both the right-hand terms of equation (16). The first term (coherence between $3d_0$ and $3d_1$) and the second term (coherence between $3d_1$ and $3d_2$) of equation (16) are shown by broken and chain curves respectively.

It is obvious that there are four real parameters entering into this expression; two of them are the relative scattering probabilities of the $m=0$ and $m=1$ components, and the other two are the relative phases between the $m=0, 1$ and 2 scattering amplitudes. In figure 9 we also show the contribution to $\langle L_y \rangle$ from the two terms on the right-hand side of equation (16): the first from the $m=0$ and $m=1$ and the second from the $m=1$ and $m=2$ amplitudes. It turns out that these two terms have opposite signs for most scattering angles and their sum contributes to the structure of the calculated $\langle L_y \rangle$. The significance and the physics of the two separate terms in equation (16) is not evident.

For comparison we have also calculated $\langle L_y \rangle$ for positron impact excitation and our results are shown in figure 10 for $X=2, 3, 4$ and 5 . We note that, unlike at lower energies ($X=2$ and 3) where the orientation is negative at all scattering angles, at higher energies it becomes positive in the forward direction and remains negative for backward scattering angles. In figure 10, we also plot the contribution from the two terms on the right-hand side of equation (16). We see that the second term is positive at all energies and angles, while the first term becomes smaller (and even positive at some middle angles) as the energy increases; this results in $\langle L_y \rangle$ being positive when $E > 3E_{th}$. It may be quite interesting to see if this behaviour also shows up in other calculations of positron impact excitation of helium.

4. Conclusions

We have presented alignment (γ) and orientation ($\langle L_y \rangle$) parameters for e^\pm impact excitation of hydrogen-like positive ions at intermediate and high energies in the Coulomb-Born approximation. The alignment and orientation for excitation to $2p$

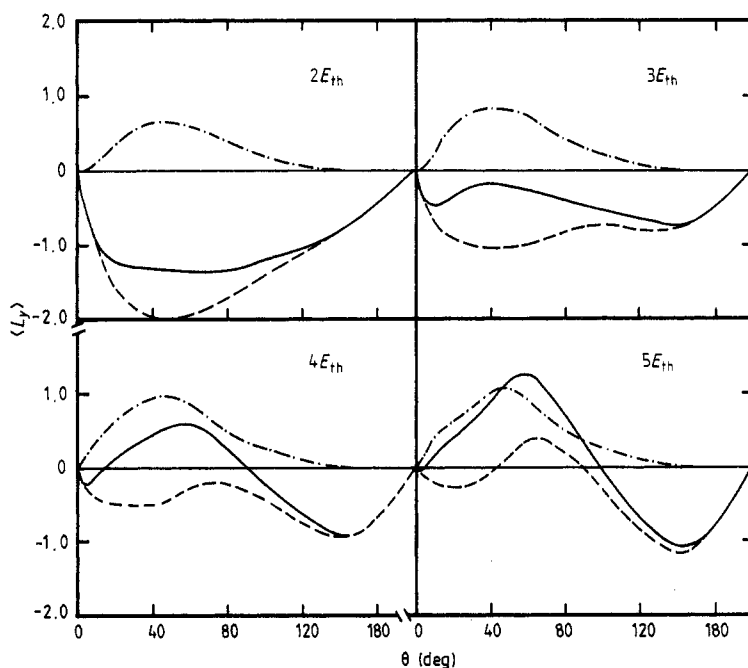


Figure 10. Same as figure 9, but for positron scattering at $2, 3, 4$ and $5E_{th}$ collision energies.

states by electron and positron impact are found to be similar to those for the corresponding excitation of neutral targets. These results contradict the simple classical grazing model where the sign of $\langle L_y \rangle$ was interpreted in terms of effective attractive or repulsive forces between the incident particle and the target. We have also examined the orientation parameter for the excitation of 3d states of He^+ by electron and positron impact. The results are quite different from those found for excitation of 2p states. This further discourages a simple classical model of the $\langle L_y \rangle$ parameter.

We have also examined the coherence between the 2s and 2p states by electron and positron impact excitation of He^+ in the Coulomb-Born approximation. From the dipole moment $\langle \mathbf{A} \rangle$ and the $\langle (\mathbf{L} \times \mathbf{A}) \rangle$ vectors one can obtain a classical orbital picture of the excited electron charge cloud. We find that the direction of the dipole moment in general is consistent with the alignment angle γ calculated from the 2p states alone and that the sense of the rotation of the electron in the classical orbital picture is consistent with the rotation $\langle L_y \rangle$ derived from the 2p states. Contour plots of the charge densities at different scattering angles are used to assist the interpretation of classical pictures derived from the calculated quantal expectation values. We have also explored the Z dependence of the $\langle L_y \rangle$ parameter for electron impact excitation to 2p states of hydrogenic ions. At the same scaled energy, the sign changeover in $\langle L_y \rangle$ occurs at almost the same scattering angle. We find some evidence that the value of $\langle L_y \rangle$ for positron impact excitation to the 3d states of hydrogen-like ions becomes positive at intermediate angles for higher energies.

Acknowledgments

This work is supported in part by the US Department of Energy, Office of Energy Research, Division of Chemical Sciences. We are thankful to Don Madison for fruitful discussions.

References

- Andersen N, Andersen T, Dahler J S, Nielsen S E, Nienhuis G and Refsgaard K 1983 *J. Phys. B: At. Mol. Phys.* **16** 817
- Andersen N, Gallagher J W and Hertel I V 1988 *Phys. Rep.* **165** 1-188
- Andersen N and Hertel I V 1986 *Comment. At. Mol. Phys.* **19** 35-58
- Bartschat K and Madison D H 1988 *J. Phys. B: At. Mol. Phys.* **21** 153-70
- Beijers J P M, Doornenbal S J, van Eck J and Heideman H G M 1987 *J. Phys. B: At. Mol. Phys.* **19** L837
- Blum K 1981 *Density Matrix, Theory and Applications* (New York: Plenum)
- Burgdörfer J 1983 *Z. Phys. A* **309** 285
- Burgdörfer J and Dube L J 1984 *Phys. Rev. Lett.* **52** 2225
- Cartwright D C and Csanak G 1987 *J. Phys. B: At. Mol. Phys.* **20** L583
- Csanak G and Cartwright D C 1986 *Phys. Rev. A* **34** 93-6
- Deb N C and Sil N C 1983 *Phys. Rev. A* **28** 2806-10
- Deb N C, Sinha C and Sil N C 1983 *Phys. Rev. A* **27** 2447-55
- Eminyan M, MacAdam K B, Slevin J and Kleinpoppen H 1974 *J. Phys. B: At. Mol. Phys.* **7** 1519
- Fano U and Macek J H 1973 *Rev. Mod. Phys.* **45** 553
- Havener C C, Rouze N, Westerveld W B and Risley J S 1986 *Phys. Rev. A* **33** 276
- Jain A, Lin C D and Fritsch W 1987a *Phys. Rev. A* **35** 3180
- 1987b *Phys. Rev. A* **36** 2041
- 1988 *J. Phys. B: At. Mol. Opt. Phys.* **21** 1545

Kohmoto M and Fano U 1981 *J. Phys. B: At. Mol. Phys.* **14** L447

Lin C D and Jain A 1988 to be published

Madison D H and Winters K H 1983 *J. Phys. B: At. Mol. Phys.* **16** 4437-50

Madison D H, Csanak G and Cartwright D C 1986 *J. Phys. B: At. Mol. Phys.* **19** 3361-6

Standage M C and Kleinpoppen H 1976 *Phys. Rev. Lett.* **36** 577

Steph N C and Golden D E 1980 *Phys. Rev. A* **21** 1848-55

Stewart M and Madison D H 1981 *Phys. Rev. A* **23** 647

van Wyngaarden W L and Walters H R J 1986 *J. Phys. B: At. Mol. Phys.* **19** 929